J|A|C|S
ARTICLES
Published on Web 02/08/2003

Different Surface Chemistries of Water on Ru{0001}: From Monomer Adsorption to Partially Dissociated Bilayers

A. Michaelides, A. Alavi, and D. A. King*

Contribution from the Department of Chemistry, University of Cambridge, Cambridge CB2 1EW, U.K.

Received October 8, 2002; E-mail: daksec@ch.cam.ac.uk

Abstract: Density functional theory has been used to perform a comparative theoretical study of the adsorption and dissociation of H_2O monomers and icelike bilayers on Ru{0001}. H_2O monomers bind preferentially at atop sites with an adsorption energy of ~0.4 eV/H_2O. The main bonding interaction is through the H_2O $1b_1$ molecular orbital which mixes with Ru $\mathbf{d}_{z^2}$ states. The lower-lying set of H_2O molecules in an intact H_2O bilayer bond in a similar fashion; the high-lying H_2O molecules, however, do not bond directly with the surface, rather they are held in place through H bonding. The H_2O adsorption energy in intact bilayers is ~0.6 eV/H_2O and we estimate that H bonding accounts for ~70% of this. In agreement with Feibelman (*Science* **2002**, *295*, 99) we find that a partially dissociated OH + H_2O overlayer is energetically favored over pure intact H_2O bilayers on the surface. The barrier for the dissociation of a chemisorbed H_2O monomer is 0.8 eV, whereas the barrier to dissociate a H_2O incorporated in a bilayer is just 0.5 eV.

1. Introduction

Water is one of the most plentiful and essential compounds occurring in nature, which makes its interaction with metal surfaces of interest to various fields of science. Its particular relevance to heterogeneous catalysis, electrochemistry, and hydrogen production for fuel cells has prompted an enormous number of studies. Nonetheless, our atomic level understanding of the structure and chemistry of water−metal interfaces remains unclear. This was aptly demonstrated recently by Feibelman's questioning of the conventional belief that water deposition on Ru produces a hexagonal icelike layer.[1]

Nondissociative H_2O adsorption on close-packed metal surfaces is thought to proceed through the adsorption of isolated H_2O monomers that quickly group to form small or extended hydrogen-bonded clusters.[2−5] On close-packed metal surfaces, in particular those with hexagonal symmetry, the most common extended overlayer is thought to be an icelike bilayer. In the archetypal bilayer, H_2O molecules arrange, as in ice I_h, in puckered hexagonal rings. The O atoms lie in two planes separated by about 1 Å (0.96 Å). H atoms belonging to the lower-lying oxygens form H bonds with neighboring water molecules. The higher-lying O atoms contribute one H to the hexagonal H bonding network and one OH bond is oriented along the surface normal. Experimental evidence exists for bilayer formation on the noble metals and most of the late 3, 4, and 5d transition metals.[6,7]

The most intensively investigated prototype system for the adsorption of water on single-crystal surfaces is water on Ru{0001}.[8−15] Until the low-energy electron diffraction (LEED) study of Held and Menzel,[12] water adsorption at low temperatures (100−200 K) on Ru{0001} was thought to be relatively well understood. However, Held and Menzel's LEED structural analysis of D_2O adsorption revealed that, although the D_2O overlayers had $(\sqrt{3} \times \sqrt{3})R30°$ periodicity, characteristic of an adsorbed bilayer, each plane of O atoms was not separated by 0.96 Å but instead by only 0.1 Å. Thus, it was proposed that a vertically *compressed* D_2O bilayer had been identified. D_2O was used in this study because slight bond length changes result in rather complicated long-range periodicity for H_2O overlayers.[13] However, similar LEED current versus voltage ($I-V$) curves were reported for H_2O and D_2O overlayers indicating that their local geometries are similar.

Recently, Feibelman performed a theoretical investigation of this system and did not identify a compressed H_2O bilayer with nearly coplanar oxygens.[1] According to his density functional theory (DFT) calculations, all pure H_2O bilayers should be buckled by at least 0.5 Å. Instead, his calculations revealed that the only overlayer with the correct $(\sqrt{3} \times \sqrt{3})R30°$ periodicity, which produced a nearly coplanar arrangement of oxygens, was

* Correspondence author. Tel.: +44 1223 336449. Fax: +44 1223 336362.

(1) Feibelman, P. J. *Science* **2002**, *295*, 99.
(2) Mitsui, T.; Rose, M. K.; Fomin, E.; Ogletrr, D. F.; Salmeron, M. *Science* **2002**, *297*, 1850.
(3) Morgenstern, K.; Nieminen, J. *Phys. Rev. Lett.* **2002**, *88*, 066102.
(4) Nakamura, M.; Ito, M. *Chem. Phys. Lett.* **2000**, *325*, 293.
(5) Nakamura, M.; Shingaya, Y.; Ito, M. *Chem. Phys. Lett.* **1999**, *309*, 123.
(6) Thiel, P. A.; Madey, T. E. *Surf. Sci. Rep.* **1987**, *7*, 211.
(7) Henderson, M. A. *Surf. Sci. Rep.* **2002**, *46*, 1.
(8) Doering, D. L.; Madey, T. E. *Surf. Sci.* **1982**, *123*, 305.
(9) Thiel, P. A.; dePaola, R. A.; Hoffmann, F. M. *J. Chem. Phys.* **1984**, *80*, 5326.
(10) Schmitz, P. J.; Polta, J. A.; Chang, S.-L.; Thiel, P. A. *Surf. Sci.* **1987**, *186*, 219.
(11) Pirug, G.; Ritke, C.; Bonzel, H. P. *Surf. Sci.* **1991**, *241*, 289.
(12) Held, G.; Menzel, D. *Surf. Sci.* **1994**, *316*, 92.
(13) Held, G.; Menzel, D. *Phys. Rev. Lett.* **1994**, *74*, 4221.
(14) Held, G.; Menzel, D. *Surf. Sci.* **1995**, *327*, 301.
(15) Lilach, Y.; Romm, L.; Livnech, T.; Asscher, M. *J. Phys. Chem. B* **2001**, *105*, 2736.

10.1021/ja028855u CCC: $25.00

one that consisted of equal amounts OH and H_2O. This "partially dissociated" overlayer was also about 0.2 eV/H_2O more stable than the buckled pure H_2O bilayers. Thus, it was suggested that the wetting layer observed on Ru{0001} consisted of a half-dissociated hydroxyl-water overlayer. A very recent DFT study on Pt{111}, however, finds that on this surface intact H_2O bilayers are stable compared to partially dissociated overlayers.[16] On *O covered* Pt{111}, a similar partially dissociated overlayer, but without chemisorbed H atoms, produced from H_2O and O disproportionation, had previously been theoretically predicted.[17]

Feibelman's study provided compelling evidence for a partial dissociation model on Ru{0001}, and it has already inspired several experimental reinvestigations of this system.[18,19] However, as pointed out by Menzel,[20] difficulties with this new theoretical interpretation remain. One crucial aspect of the model that remains unexplored is the *kinetic* viability of the formation of a partially dissociated overlayer. By comparing the stability of various pure H_2O and partially dissociated overlayers, Feibelman's study demonstrated that it was *thermodynamically* feasible. It is not known, however, how H_2O dissociation occurs on Ru or what the barriers might be. This is another issue well suited to density functional calculations with recent studies revealing that DFT is now a reliable tool for the determination of reaction pathways and barriers, including those involving H_2O molecules.[21−23]

In this study, we use DFT to investigate the adsorption and dissociation of H_2O monomers and icelike bilayers on Ru{0001}. Although we aim to shed some light on the issue of water adsorption on Ru{0001}, our primary goal is to understand the microscopic interactions between a transition-metal substrate and H_2O monomers and icelike bilayers. This is the first time that DFT has been used to investigate the dissociation of H_2O monomers on Ru and the dissociation of icelike bilayers on any metal surface. Some details of our first principles total energy calculations are outlined below. Structures and energetics for the adsorption and dissociation of H_2O monomers and icelike bilayers are then presented. In section 4, we discuss our results, paying particular attention to the electronic structure of H_2O adsorption, before reaching our conclusions.

2. Calculation Details

First-principle total energy calculations within the DFT framework were performed with the CASTEP code.[24] Ultrasoft pseudopotentials were expanded within a plane wave basis set up to a cutoff energy of 340 eV.[25,26] Electron exchange and correlation effects were described by the Perdew Wang 1991 (PW91)[27] generalized gradient approximation. A Fermi smearing of 0.2 eV was utilized and the corrected energy extrapolated to zero Kelvin.

The Ru{0001} surface was modeled by a periodic array of five-layer-thick Ru slabs. To minimize interactions between neighboring slabs, a vacuum region equivalent to 10 layers of Ru (~21 Å) was used. The adsorption and dissociation of H_2O monomers were investigated by placing a single H_2O in a p(2 × 2) unit cell. Additional calculations on the H_2O monomer were also performed in a larger p(3 × 3) unit cell. To be consistent with the experimentally observed periodicity for D_2O overlayers, H_2O bilayers and their dissociation products were examined in $(\sqrt{3} \times \sqrt{3})$R30° and $(2\sqrt{3} \times 2\sqrt{3})$R30° unit cells. A Monkhorst−Pack[28] mesh with 4 × 4 × 1 k-point sampling within the surface Brillouin zone was used for the $(\sqrt{3} \times \sqrt{3})$R30° cell and varied accordingly for the others.

In all optimizations of stable structures, the bottom four Ru layers were fixed at their ab initio bulk-truncated positions (a = 2.720 Å (expt = 2.706[29]), c = 4.289 Å (expt = 4.282[29])) and the remaining atoms were allowed to fully relax. Structure optimizations of elementary reaction steps and molecular rearrangements were investigated by applying additional constraints to the adsorbates. In particular, reaction pathways were investigated by constraining O−H bonds at fixed distances and then minimizing the total energy with respect to all remaining degrees of freedom. Through a series of such structure optimizations, using a different reactant separation in each case, we determine an energy profile for the reaction.[30,31] Since, in this approach, the only constraint on the reactants is the O−H distance, they are otherwise free to rotate and translate. A transition state is identified when the forces on the ions are zero (i.e., fall below a given tolerance level) and the configuration corresponds to a maximum in the energy with respect to the reaction coordinate and a minimum with respect to all remaining ionic degrees of freedom.

Adsorption energies (E_{ads}) are calculated from

$$E_{ads} = E_A + E_{Ru} - E_{A/Ru} \quad (1)$$

where E_A, E_{Ru}, and $E_{A/Ru}$ are the total energies of the isolated adsorbate, the clean Ru{0001} surface, and the chemisorption system, respectively. In this definition, positive adsorption energies correspond to an exothermic adsorption process. The reference energies of the isolated gas-phase adsorbates are calculated by placing them in a 12 Å^3 cell. For the isolated OH and H species in the gas phase, their energies are obtained from spin-polarized (GGS) calculations.

3. Results

3.1. H_2O Monomer Adsorption and Dissociation. (a) H_2O Monomer Adsorption. The adsorption of a H_2O monomer at the four high-symmetry sites (hcp, fcc, bridge, and atop) of Ru{0001} was investigated. Adsorption energies and optimized structural parameters at each site are listed in Table 1. It can be seen that the most stable site for H_2O, with an adsorption energy of 0.38 eV, is the atop site. Each of the other sites are strongly disfavored with binding energies of approximately 0.1 eV or less. The preferred structure of H_2O at the atop site is shown in Figure 1a. In agreement with experiment and with recent DFT calculations on Pt{111}, H_2O preferentially lies nearly parallel to the surface.[4,22] The angle between the H_2O dipole plane and the Ru surface is 6°. At this site on Ru{0001}, the O−Ru distance is quite long at 2.29 Å and the internal structure of the H_2O monomer is only moderately deformed.

The favored azimuthal orientation identified for H_2O at the atop site has one OH bond directed toward an hcp site and the

(16) Meng, S.; Xu, L. F.; Wang, E. G.; Gao, S. *Phys. Rev. Lett.* **2002**, *89* 176104.
(17) Michaelides, A.; Hu, P. *J. Chem. Phys.* **2001**, *114*, 513.
(18) Puisto, S. R.; Lerotholi, T. J.; Held, G.; Menzel, D. *Surf. Rev. Lett.* In press.
(19) Denzler, D. N.; Wagner, S.; Wolf, M.; Ertl, G. *Surf. Sci.* In press.
(20) Menzel, D. *Science* **2002**, *295*, 58.
(21) Greeley, J.; Nørskov, J. K.; Mavrikakis, M. *Annu. Rev. Phys. Chem.* **2002**, *53*, 319.
(22) Michaelides, A.; Hu, P. *J. Am. Chem. Soc.* **2001**, *123*, 4235.
(23) Marx, D.; Tuckerman, M. E.; Hutter, J.; Parrinello, M. *Nature* **1999**, *397*, 601.
(24) Payne, M. C.; Teter, M. P.; Allan, D. C.; Arias, T. A.; Joannopoulos, J. D. *Rev. Mod. Phys.* **1992**, *64*, 1045.
(25) Vanderbilt, D. *Phys. Rev. B* **1990**, *41*, R7892.
(26) For increased accuracy, the Ru pseudopotential explicitly includes semicore 4s and 4p states as valence states. Thus, a total of 16 valence electrons on Ru were treated within the calculations.
(27) Perdew, J. P.; Chevary, J. A.; Vosko, S. H.; Jackson, K. A.; Pederson, M. R.; Singh, D. J.; Fiolhais, C. *Phys. Rev. B* **1992**, *46*, 6671.
(28) Monkhorst, H. J.; Pack J. D. *Phys. Rev. B* **1976**, *13*, 5188.
(29) *Handbook of Chemistry and Physics*, 80th ed.; Lide, D. R., Ed.; CRC: London, 1999.
(30) Alavi, A.; Hu, P.; Deutsch, T.; Silvestrelli, P. L.; Hutter, J. *Phys. Rev. Lett.* **1998**, *80*, 3650.
(31) Michaelides, A.; Hu, P. *J. Chem. Phys.* **2000**, *112*, 8120.

Table 1. Adsorption Energies and Optimized Structural Parameters for a H_2O Monomer at the Four High-Symmetry Sites of Ru{0001}[a]

site	E_{ads} (eV)	O–Ru (Å)	O–H (Å)	Surf-O–H (°)	H–O–H (°)
atop	0.38 (0.35)[b]	2.29	0.99, 0.98	98, 89	106
bridge	0.12	2.54, 2.58	0.98, 0.98	129, 120	111
fcc	0.05	3.12, 3.17, 3.26	0.98, 0.98	74, 89	105
hcp	0.04	3.00, 3.06, 3.08	0.98, 0.98	76, 81	104
gas phase			0.97 (0.96)[c]		105.2 (104.5)[c]

[a] All values, unless otherwise stated, are for a (2 × 2) unit cell. For reference purposes, the calculated and experimental bond length and internal angle of a gas-phase H_2O are also given. [b] $(\sqrt{3} \times \sqrt{3})R30°$ unit cell. [c] Experimental values (ref 29).

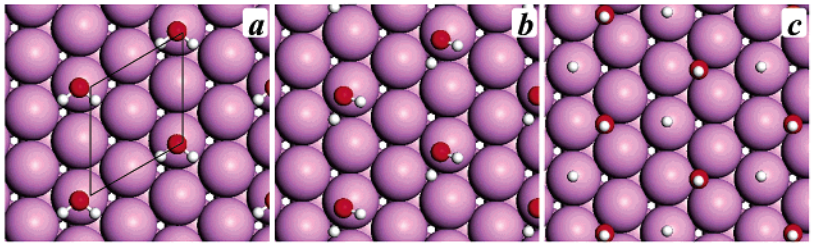

Figure 1. Structures of the initial (a), transition (b), and final states (c), of H_2O monomer dissociation on Ru{0001}. The parallelogram in (a) indicates the surface, p(2 × 2), unit cell.

other close to the direction of a bridge site. This is not a strong preference, however, since the potential energy surface (PES) for rotation about the surface normal at this site is flat with a maximum barrier of ~0.02 eV.

(b) H_2O Monomer Dissociation. We now turn our attention to reaction pathways for the dissociation of the H_2O monomer. Since it is possible that H_2O diffuses away from its favored atop site before dissociating, reaction pathways with H_2O initially adsorbed at three-fold and bridge sites were examined in addition to two channels with H_2O at the atop site. We know that the reactants are free to rotate and translate across the surface unit cell. Therefore, the reaction channels serve merely as initial guesses to the pathway. The reactants are in no way constrained to their initial channels. Indeed, we find that the four initial channels yield just two distinct transition states. The lowest energy transition state of these two (Figure 1b) has O (OH) located close to an atop site and the dissociating H is near an fcc site, 1.45 Å from the O. The other transition state (not shown) is 0.1 eV higher in energy and has OH located over a three-fold site. Relative to H_2O chemisorbed at the atop site, the activation energy for the dissociation of a H_2O monomer through the lowest energy transition state is 0.80 eV.

To get a more accurate value for the dissociation barrier of the H_2O monomer, H_2O dissociation was also examined in a (3 × 3) cell. In the larger cell, the H_2O-H_2O separation between molecules in adjacent cells is much greater and any self-interaction between H_2O molecules will be reduced. The calculated barrier we get in the (3 × 3) cell is 0.85 eV, slightly higher than that obtained in the (2 × 2) cell. The structure of the transition state in the (3 × 3) cell is nearly identical to that identified in the (2 × 2) cell.

(c) H_2O Monomer Dissociation Products. The final state of the H_2O dissociation reaction in the (2 × 2) cell is shown in Figure 1c and the optimized structural parameters are given in Table 2. This corresponds to the most stable coadsorption of OH and H in the (2 × 2) unit cell. It has OH adsorbed at an fcc site and H at an atop site. This coadsorbed state is at essentially the same energy as the chemisorbed H_2O initial state, revealing that the dissociation reaction in the (2 × 2) cell is thermoneutral (enthalpy change (ΔH) = 0.00 eV to within the accuracy of the present calculations).

Table 2. Adsorption Energies and Optimized Structural Parameters for OH and H Adsorption and OH + H Coadsorption in p(2 × 2) Unit Cells on Ru{0001}[a]

	OH E_{ads} (eV)	O–Ru (Å)	O–H (Å)	Surf-O–H (°)	H E_{ads} (eV)	H–Ru (Å)
hcp	3.10	2.19, 2.20, 2.21	0.97	179	2.72	1.90, 1.92, 1.94
fcc	3.21	2.20, 2.20, 2.21	0.97	179	2.79	1.85, 1.90 2.00
bridge	3.10	2.15, 2.19	0.98	136	2.64	1.81, 1.80
atop	2.82	1.97	0.98	128	2.48	1.63
OH + H		2.16, 2.19, 2.21	0.98	175		1.64

[a] The OH + H coadsorbed state, shown in figure 1c, has OH at an fcc site and H at an atop site of the fourth Ru atom in the p(2 × 2) surface unit cell.

In practice, however, OH and H will not be constrained to the artificial confines of the (2 × 2) unit cell and will be free to diffuse away from each other, possibly altering the energy of the final state. To investigate this, the separate adsorption of OH and H in p(2 × 2) unit cells was examined. The calculated adsorption energies and optimized structural parameters of OH and H at each of the high symmetry sites on Ru{0001} are given in Table 2. We find that both OH and H bind most strongly at fcc three-fold hollow sites with adsorption energies of 3.21 and 2.79 eV, respectively. For H, where comparison is available, this agrees with experimental and previous theoretical findings.[32,33] Taking together the chemisorption of OH and H in separate (2 × 2) unit cells, the enthalpy change for the dissociation of chemisorbed H_2O is −0.27 eV. This reveals that 0.27 eV is gained between the (2 × 2) coadsorbed final state, Figure 1c, and the separate (2 × 2) chemisorption states. This energy gain occurs mainly because H is forced to sit at an unfavorable atop site in the coadsorption system. Moreover, the −0.27 eV enthalpy change reveals that thermodynamically there is a driving for the H_2O monomer to dissociate, although as we have seen, it is kinetically hindered to do so. The complete energy profile for the adsorption and dissociation of the H_2O monomer is shown in Figure 2.

3.2. H_2O Bilayer Adsorption and Dissociation. H_2O adsorption and dissociation were then investigated in ice bilayer

(32) Barteau, M. A.; Broughton, J. Q.; Menzel, D. *Surf. Sci.* **1983**, *133*, 443.
(33) Feibelman, P. J.; Hamann, D. R. *Surf. Sci.* **1987**, *179*, 153.

Table 3. Adsorption Energies and Optimized Structural Parameters for Pure H_2O Bilayers and $OH-H_2O$ ("Partially Dissociated") and 2OH ("Fully Dissociated") Overlayers on Ru{0001}[a]

	E_{ads} (eV/H_2O)	Δ(O–O)(Å)[b]	O–Ru (Å)	O–H (Å)	O–H_{bond} (Å)	ΔRu (Å)[c]
$2H_2O$ (H-up) (Figure 3a)	0.58 (0.52)	0.74 (0.72)	2.50, 3.31	0.97, 0.99, 0.99, 1.01	1.72, 1.87, 1.89	0.06
$2H_2O$ (H-down) (Figure 3b)	0.57 (0.53)	0.51 (0.52)	2.45, 3.10	0.99, 0.99, 0.99, 1.01	1.76, 1.80, 1.82	0.13
atop-H + OH + H_2O (Figure 3d)	0.78 (0.71)	0.05 (0.05−0.06)	2.07, 2.17 (2.09, 2.16)	0.99, 1.02, 1.02	1.65, 1.68, 1.98	0.14 (0.14)
OH + H_2O	1.00 (0.96)	0.06 (0.06)	2.12, 2.19	0.98, 1.02, 1.02	1.64, 1.67, 1.99	0.06
2OH	0.66	0.00	1.96, 1.96	1.01, 1.00	1.64, 1.80	0.09
experiment		0.09[d]	2.06, 2.23[d]			0.07[d]
		0.07[e]	2.05, 2.20[e]			0.14[e]

[a] Where direct comparison is possible, Feibelman's values (ref 1) are given in parenthesis. [b] O−O buckling. [c] Ru surface layer buckling. [d] Ref 12 (Held and Menzel). [e] Ref 18 (Puisto et al.).

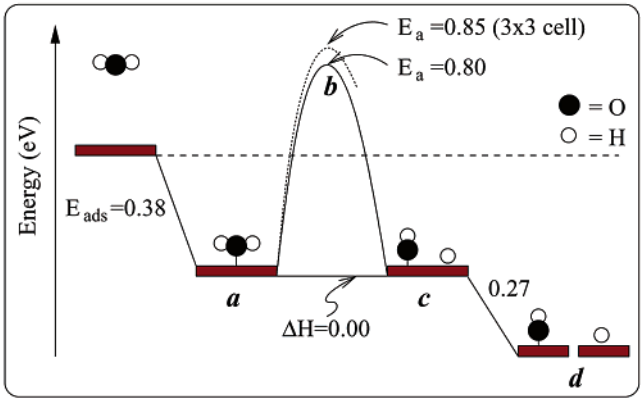

Figure 2. Relative energy diagram for H_2O monomer adsorption and dissociation on Ru{0001}. The states labeled a, b, and c correspond to the structures shown in figure 1a, 1b, and 1c, respectively. State d corresponds to OH and H chemisorbed in separate unit cells. All energies, unless indicated otherwise, are for a p(2 × 2) unit cell.

structures on Ru{0001}. As discussed in the Introduction, the typical intact H_2O bilayer consists of puckered hexagonal rings of triply H-bonded molecules. In this overlayer, every second H_2O molecule lies fairly flat on the surface, and the remaining H_2O molecules lie further from the surface with one OH bond in the surface normal. This non-hydrogen-bonded OH bond can point either away from the surface (H-up) or toward the surface (H-down). Feibelman suggested that on Ru{0001} this OH bond is broken, resulting in a partially dissociated H_2O-OH bilayer and adsorbed H atoms.[1] We have looked again at these pure and partially dissociated bilayers and have examined mechanisms for their interconversion. A "fully dissociated" (2OH) overlayer was also investigated.

(a) Intact H_2O Bilayer Adsorption. Optimized structural parameters and adsorption energies for H-up and H-down pure intact H_2O bilayers are listed in Table 3 and their structures are shown in Figure 3a and b, respectively. Notably, in agreement with Feibelman, the buckling between O layers (Δ(O−O) in Table 3) in pure H_2O bilayers is always large, ∼0.5 and ∼0.7 Å in H-up and H-down bilayers, respectively. Several calculations using initially coplanar or nearly coplanar arrangements of oxygens were performed. Each of these, however, optimized to highly buckled bilayers. Thus, although the intact bilayers identified here are somewhat compressed compared to an ideal ice I_h bilayer (Δ(O−O)-ice ∼0.96 Å), they still prove inconsistent with the experimentally observed small (∼0.1 Å) buckling.[12]

Our calculated adsorption energies of 0.58 and 0.57 eV/H_2O for the H-up and H-down bilayers agree well with Feibelman's values of ∼0.53 eV. As pointed out by Feibelman, this puts the calculated H_2O adsorption energy on Ru{0001} about 0.1−0.2 eV less than the calculated values for the sublimation energy of bulk ice.[1] This implies, it was argued, that intact H_2O molecules should not wet the Ru{0001} surface but rather form 3-D ice. However, it remains to be seen if the relevant comparison should be with *bulk* ice or rather with finite-sized H_2O clusters. Moreover, on Pt{111} where the calculated H_2O adsorption energy in a bilayer, 0.53 eV,[16] is similar to that on Ru{0001}, it is known that the preparation conditions (temperature, pressure, H_2O dosing rate[34]) are very important in determining whether 2-D wetting layers or 3-D ice crystals form Clearly, a delicate balance between 2-D and 3-D ice growth exists on Pt{111} and it remains to be seen if any DFT comparison of equilibrium structures can conclusively say whether intact H_2O bilayers cannot form under experimental conditions at finite temperatures and pressures.

In the intact bilayers, both types of H_2O are located over atop sites. The lower set lies quite flat on the surface, in a manner similar to that of a H_2O monomer; the higher-lying H_2O molecules sit upright in the plane of the surface normal. Both types of H_2O molecule are reasonably far from the surface. In the H-up bilayer, for example, the shortest O−Ru distances are 2.50 and 3.31 Å for the low- and high-lying H_2O molecules, respectively. Notably, then, the low-lying H_2O molecules in an adsorbed bilayer sit >0.2 Å further from the surface than an isolated H_2O monomer does. The high-lying set of H_2O molecules has apparently "pulled" the low-lying H_2O molecules away from the surface. The three O−H bonds involved in H-bonding tend to be lengthened slightly to 0.99−1.01 Å and the H···O H-bonding distances are in the 1.7−1.9 Å range. The non-H-bonded O−H bond is only 0.97 Å in the H-up bilayer, while in the H-down bilayer it is 1.01 Å, indicating an interaction between this H and the Ru surface in the H-down bilayer.

(b) H-Up/H-Down Bilayer Interconversion. We have established that the H-up and H-down intact bilayers have a similar energy. This raises an interesting question, whether the conversion between H-up and H-down bilayers proceeds with ease. This process may be important in bilayer dissociation. Two possible mechanisms for it have been examined. The first involved rotating the OH-up bond of the high-lying H_2O toward the surface within the plane of the molecule; the second involved a rotation of the OH-up bond perpendicular to the plane of this H_2O. A schematic diagram illustrating these two processes is shown in Figure 4. We find that the first mechanism has a barrier of 0.30 eV. The second is more kinetically hindered with a barrier of 0.80 eV. Apparently, the second mechanism is costly because it goes through a state which essentially has two hydrogens between two oxygens. Although even the first

(34) Glebov, A.; Graham, A. P.; Menzel, A.; Toennies, J. P. *J. Chem. Phys.* **1997**, *106*, 9382.

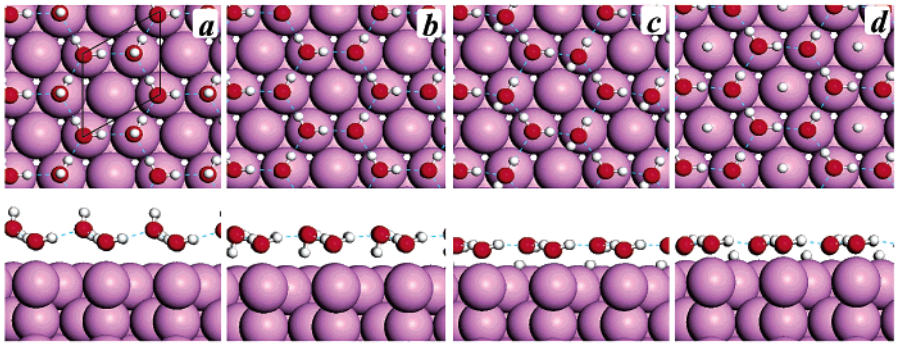

Figure 3. Top and side views of (a) "H-up" intact bilayer, (b) "H-down" intact bilayer, (c) the transition state for bilayer dissociation, and (d) the partially dissociated OH−H_2O+H overlayer. The parallelogram in (a) indicates the surface, ($\sqrt{3} \times \sqrt{3}$)R30°, unit cell.

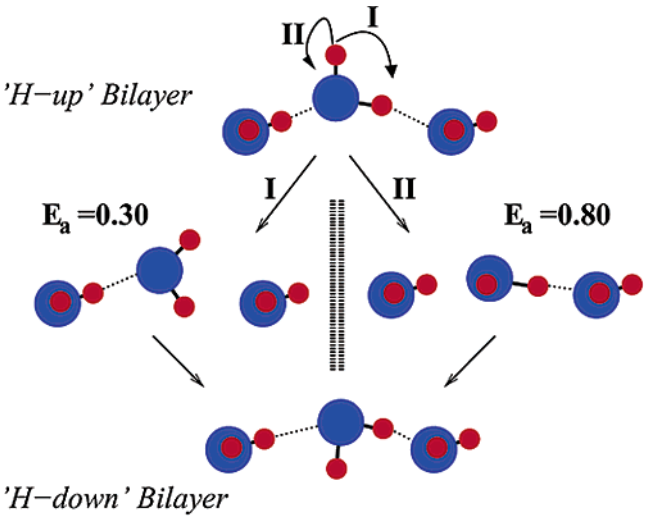

Figure 4. A schematic diagram (side view) illustrating the two mechanisms investigated for the conversion of a "H-up" into a "H-down" intact bilayer on Ru{0001}. For clarity, the Ru surface is not shown.

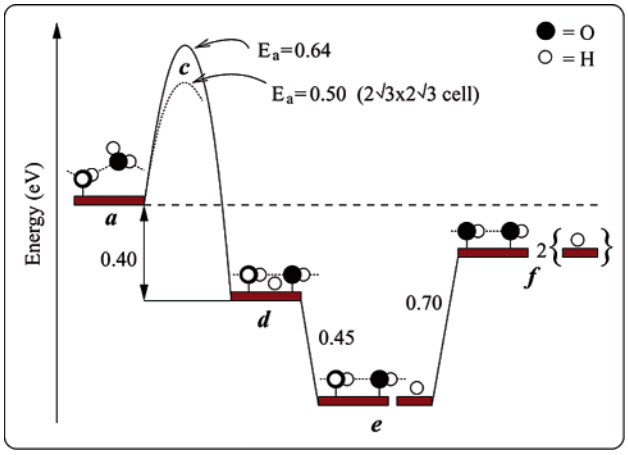

Figure 5. Relative energy diagram for H_2O bilayer adsorption and dissociation on Ru{0001}. States a, c, and d correspond to the structures shown in figures 3a, 3c, and 3d, respectively. e corresponds to the energy of the OH−H_2O overlayer with the chemisorbed H atom removed to a separate ($\sqrt{3} \times \sqrt{3}$)R30° unit cell. f is the pure OH "fully dissociated" overlayer. The relative energy of this state has been calculated by taking the sum of the adsorption energy of this overlayer and two chemisorbed H atoms, calculated in separate ($\sqrt{3} \times \sqrt{3}$)R30° unit cells. All energies, unless indicated otherwise, are for a ($\sqrt{3} \times \sqrt{3}$)R30° unit cell.

mechanism, the in-plane rotational mechanism, may not follow the minimum energy pathway for this process, its identification indicates that the transformation of a H-up H_2O into a H down H_2O is facile and could proceed on an experimental time scale at the low surface temperatures of interest (100−150 K).

(c) H_2O Bilayer Dissociation. Mechanisms for the dissociation of both the H-up and H-down intact bilayers were then considered. In addition to pathways in which each of the OH bonds were stretched in the H-up and H-down bilayers, we also investigated dissociation pathways in which certain H-surface distances were constrained. The only pathway identified, however, that leads to the desired dissociation products is where the OH bond that points toward the surface in the H-down bilayer is stretched. The transition state of this dissociation process is shown in Figure 3c. At the transition state, the O−H distance of the breaking bond is 1.34 Å and the O−Ru distance for this dissociating H_2O has reduced from an initial value of 3.10 Å to 2.53 Å. Similarly, the height of the nondissociating H_2O above the surface has reduced by about 0.2 Å. The barrier for dissociation is 0.62 eV relative to the H-down bilayer or 0.64 eV relative to the slightly more stable (H-up) bilayer (Figure 5).

Given that we have periodic boundary conditions, it is important to recognize that the transition-state structure for bilayer dissociation corresponds to a periodic array of transition states on the surface. Since there are two H_2O molecules per ($\sqrt{3} \times \sqrt{3}$)R30° unit cell, half the H_2O molecules on the surface (or half the H_2O molecules in every hexagon) are dissociating simultaneously. This may, of course, represent an unrealistic over-constrained scenario. In practice, if dissociation of an intact bilayer is to occur, it is more likely that individual H_2O molecules dissociate at different times. To investigate the situation where no more than one H_2O in a hexagon of an adsorbed bilayer dissociates, we have examined H_2O dissociation in a much larger ($2\sqrt{3} \times 2\sqrt{3}$)R30° unit cell. The barrier we find for the dissociation of just one of the eight H_2O molecules in this cell is 0.50 eV (relative to the H-up bilayer). This is 0.14 eV less than the barrier obtained in the ($\sqrt{3} \times \sqrt{3}$)R30° unit cell. Thus, the more realistic process in the larger unit cell with many more degrees of freedom proceeds more readily. The structure of the dissociating H_2O at the transition state in the ($2\sqrt{3} \times 2\sqrt{3}$)R30° cell is essentially the same as that obtained in the ($\sqrt{3} \times \sqrt{3}$)R30° unit cell. The major structural difference lies in the H_2O molecules adjacent to the dissociating H_2O. At the transition state in the ($2\sqrt{3} \times 2\sqrt{3}$)-R30° cell, these H_2O molecules remain close to the equilibrium positions, unlike in the ($\sqrt{3} \times \sqrt{3}$)R30° cell where the nondissociating H_2O moved ~0.2 Å closer to the surface. Obviously, in the larger cell after dissociation of this first high-lying H_2O molecule there remain other high-lying H_2O mol-

ecules that must dissociate to produce the final 50:50 OH−H_2O. The mechanisms for these subsequent dissociation steps have not yet been determined and it remains to be seen if they too will have barriers of ∼0.5 eV.

When we compare the most accurate barriers for the dissociation of a H_2O monomer and a H_2O incorporated in a bilayer, that is, 0.85 eV for the monomer in the (3 × 3) cell and 0.50 eV for the bilayer in the ($2\sqrt{3} \times 2\sqrt{3}$) cell, we see that it is substantially easier to dissociate a H_2O incorporated in a bilayer than it is to dissociate an isolated chemisorbed H_2O. This significant decrease in the H_2O dissociation barrier, which we will return to in section 4, is an unexpected finding of this study.

(d) H_2O Bilayer Dissociation Products: OH−H_2O and H. The product of the bilayer dissociation reaction in the ($\sqrt{3} \times \sqrt{3}$) unit cell is shown in Figure 3d. This is the OH−H_2O+H partially dissociated bilayer model for H_2O adsorption suggested by Feibelman.[1] The adsorption energy and optimized structural parameters of this overlayer are given in Table 3. In agreement with Feibelman's calculations, we find that the partially dissociated overlayer is 0.2 eV/H_2O more stable than the pure H_2O bilayers. Thus, the dissociation of a single H_2O molecule in a H_2O bilayer to produce coadsorbed OH−H_2O+H is exothermic by 0.4 eV. In this overlayer OH, H_2O, and H each adsorb at atop sites. The H_2O and OH form hydrogen-bonded hexagonal networks and in the center of each hexagon is a chemisorbed H atom. If the chemisorbed H atom is removed from the cell and allowed to adsorb at its preferred fcc site in a separate ($\sqrt{3} \times \sqrt{3}$)R30° unit cell, a further 0.45 eV can be gained, rendering the dissociation reaction 0.85 eV exothermic. However, in practice it is not known if this final H removal step is possible. To take place, it requires that there are clean patches of Ru and that the barrier to H diffusion out of the OH−H_2O overlayer is not prohibitively large.

The structure of the OH−H_2O overlayer, with a nearly coplanar arrangement of oxygens (Δ(O−O) = 0.05−0.06 Å) and O−Ru distances of 2.1 and 2.2 Å, is in much better agreement with Held and Menzel's experimental structure than any of the pure H_2O overlayers.[12] Indeed, a refined structural analysis of Held and Menzel's *I*−*V* curves recently performed by Puisto at al.[18] brings the experimental and DFT structures into even closer correspondence (Table 3).

There have been some subtle bond length changes upon formation of the partially dissociated overlayer. First, the O−Ru distance for the H_2O molecule in this overlayer is 2.20 Å. This is about 0.1 Å *shorter* than the Ru−O distance for an adsorbed H_2O monomer (2.29 Å). Although, on going from an adsorbed monomer to a pure H_2O bilayer, H_2O moved away from the surface, what we see here is the opposite effect: On adsorbing a OH next to a H_2O, the H_2O moves closer to the surface. Second, the OH−Ru distance of 2.09 Å is about 0.1 Å *longer* than the equilibrium O−Ru bond length for an atop site OH (1.97 Å). The net effect of the H_2O moving toward the surface and the OH moving away from the surface is that the buckling between these adsorbates is minimized. It is not clear what the driving force for this cooperative movement is. One outcome will certainly be enhanced H bonding. Finally, with regard to H bonding, we find that the O−H bonds in H_2O are stretched to 1.02 Å, noticeably longer than the O−H bond in hydroxyl (0.99 Å). In line with this, the H bonding distances between the H_2O hydrogens and hydroxyl (1.64 and 1.67 Å) are shorter than the corresponding distance for hydroxyl (1.99 Å). This reveals that H_2O is acting as a better H bond donor than acceptor, or, conversely, hydroxyl is acting as a better H bond acceptor than donor.

(e) What about Complete Dissociation? Given that LEED is barely sensitive to the presence of H or D atoms and has not been able to discriminate between OH and H_2O, it is possible that the observed structure may not be pure H_2O or even a partially dissociated OH+H_2O overlayer but rather a "fully dissociated" 2OH+2H overlayer, that is, an overlayer in which both types of H_2O have dissociated. Indeed, on Pt{111} it has been shown that the most stable OH overlayer has ($\sqrt{3} \times \sqrt{3}$)-R30° periodicity with coplanar hydroxyls adsorbed at atop sites.[17] Structurally then this is another likely candidate for the experimentally observed overlayer.

We have investigated a 2OH−($\sqrt{3} \times \sqrt{3}$)R30° overlayer with hydroxyls adsorbed at atop sites on Ru{0001}. The adsorption energy and optimized structural parameters for this overlayer are listed in Table 3. We find, however, that the structural agreement between this overlayer and the LEED experiments is worse than that found for the OH−H_2O overlayer. The O−Ru distances are too short at 1.96 Å and the O−O buckling is too small (0.00 Å). Moreover, the fully dissociated 2OH overlayer is energetically less stable than the partially dissociated overlayer. Taking together the energies of a 2OH−($\sqrt{3} \times \sqrt{3}$)-R30° overlayer and two chemisorbed H atoms in separate ($\sqrt{3} \times \sqrt{3}$)R30° unit cells, we calculate an adsorption energy, referenced to H_2O, of 0.73 eV/H_2O. Although this overlayer is more stable than the pure H_2O bilayers, it is 0.27 eV/H_2O less stable than the equivalent OH−H_2O−($\sqrt{3} \times \sqrt{3}$)R30° plus H−($\sqrt{3} \times \sqrt{3}$)R30° partially dissociated overlayer. Thus, there is both a structural and energetic case for ruling out a fully dissociated overlayer as a model for Held and Menzel's structure.

4. Discussion

We shall now examine the electronic structure of the H_2O monomer and the intact bilayer adsorption systems. Following this, we will compare each dissociation reaction and then consider what implications our results have for the possibility of a partially dissociated overlayer on Ru.

4.1. Electronic Structure. (a) H_2O Monomer Adsorption. First, we briefly consider the occupied molecular orbitals of an isolated gas-phase H_2O. These are shown schematically in Figure 6a alongside an energy level diagram. In order of increasing energy, the occupied molecular orbitals of H_2O are labeled $\mathbf{2a_1}$, $\mathbf{1b_2}$, $\mathbf{3a_1}$, and $\mathbf{1b_1}$.[35] The $\mathbf{2a_1}$ orbital is mainly a combination of O *2s* and H **s** orbitals. This along with the $\mathbf{1b_2}$ orbital, which is a combination of an O **p** and H **s** orbitals, constitute the main H_2O bonding orbitals. The two remaining O **p** orbitals form the $\mathbf{3a_1}$ and $\mathbf{1b_1}$ orbitals. These are the highest energy occupied orbitals of H_2O. Because the $\mathbf{3a_1}$ orbital is a mixed orbital with some O and H **s** character, it resides some 2 eV below the $\mathbf{1b_1}$ orbital (Figure 6a). A partial density of

(35) The O 1s core orbital ($1a_1$) is several hundred eV below the occupied molecular orbitals of H_2O and out of the range of Figure 6. The unoccupied antibonding $2b_2$ and $4a_1$ orbitals which reside about 7 eV above the $1b_1$ orbital are also not shown.

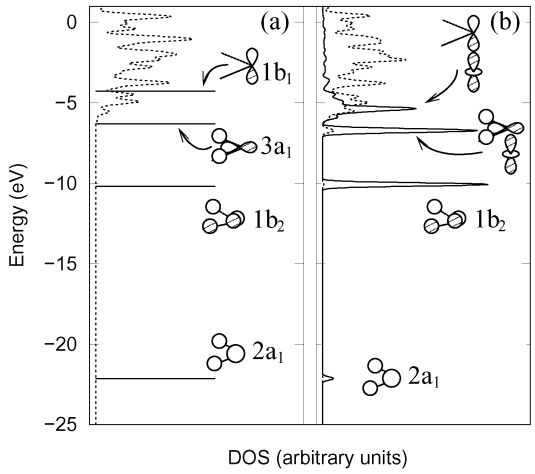

Figure 6. (a) Orbital energy diagram for gas-phase H_2O and a partial density of states (DOS) (dotted line) projected onto the **d** orbitals of a surface layer Ru atom. (b) Partial DOS projected onto the O **p** orbitals for H_2O adsorbed on Ru{0001}. The dotted line is a partial DOS projected onto the **d** states of the Ru atom bonded to H_2O. The Fermi level is zero and the H_2O levels in (a) have been shifted so that the $\mathbf{2a_1}$ peaks in (a) and (b) coincide.

states[36] (PDOS) plot projected onto the **d** orbitals of a Ru surface atom is also shown in Figure 6a.

Let us now turn our attention to the adsorption system. Figure 6b displays a PDOS plot projected onto the O **p** orbitals for a H_2O monomer adsorbed at the atop site on Ru{0001}. A PDOS projected onto the **d** orbitals (dotted line) of the Ru surface atom beneath H_2O is also displayed in Figure 6b. Three clear peaks in the O PDOS are visible at −10.1 eV, −6.8 eV, and −5.4 eV. A fourth smaller peak at −22.1 eV is also discernible. By examining the real space distribution of the individual quantum states in this system, the nature of the states within each peak has been determined. In order of increasing energy, states in the lowest energy peak (−22.1 eV) are, as in an isolated H_2O, of $\mathbf{2a_1}$ character. These states show up as a little peak in the O **p** PDOS because they are mainly **s** with only a little **p** character. In the adsorption system, they remain localized on H_2O and do not undergo any obvious interaction with the surface (Figure 7a). For the purposes of estimating how the other energy levels shift upon adsorption, we have aligned the energy of the gas-phase H_2O $\mathbf{2a_1}$ level in Figure 6a to the energy of this $\mathbf{2a_1}$ derived peak in Figure 6b. With this energy reference, the next highest energy peak (−10.1 eV) is essentially at the same energy as the gas phase $\mathbf{1b_2}$ peak. An examination of the quantum states within this peak confirms that they are indeed of $\mathbf{1b_2}$ character and again remain localized on H_2O. Like the $\mathbf{2a_1}$ derived states, the $\mathbf{1b_2}$ orbitals do not visibly interact with the surface (Figure 7b). The third peak at −6.8 eV in the adsorption system, however, is about 1 eV below the energy of the gas phase $\mathbf{3a_1}$ orbital. This energy shift is an indication that the $\mathbf{3a_1}$ orbital interacts with the surface and a visual inspection of the states within the peak confirms this.[37] A typical example of a quantum state within this peak is shown in Figure 7c. The $\mathbf{3a_1}$ derived quantum states are delocalized toward the surface and mix with Ru states. A small resonance at the energy of this peak in the Ru **d** orbital PDOS (Figure 6b) demonstrates that it is the Ru **d** orbitals with which the $\mathbf{3a_1}$ orbital mixes. A close examination of the density distributions within these $\mathbf{3a_1}$ derived quantum states reveals that it is the Ru $\mathbf{d_{z^2}}$ orbitals (not discernible from Figure 7c) that participate in these mixed orbital quantum states. Moving now to the fourth peak at −5.4 eV, it is broader than the others and resides nearly 2 eV below the level of the gas phase $\mathbf{1b_1}$ orbital. Many of the states within this peak are $\mathbf{1b_1}$ derived mixed orbital states. A representative example of a quantum state from within this peak is shown in Figure 7d. This is clearly a mixed orbital bonding state between H_2O and a Ru $\mathbf{d_{z^2}}$ orbital. When compared to the other states shown in Figure 7, the extent of the H_2O−Ru mixing in this orbital is much greater. It is plausible to attribute the H_2O−Ru chemisorption bond to a large extent to arise from the $\mathbf{1b_1}$−$\mathbf{d_{z^2}}$ mixing. However, this is not the full story, since both these orbitals are occupied prior to adsorption.

An examination of the *total electron density difference* upon adsorption augments this orbital based analysis. The charge density difference upon adsorption was determined by calculating the charge density for the adsorbate system first and then for the Ru substrate and the H_2O molecule alone, each in the optimized geometry obtained for the adsorption system. The difference between the charge density distribution of the adsorption system and the sum of the distribution for the Ru substrate and the H_2O adsorbate

$$\rho(\mathrm{Ru} + \mathrm{H_2O}) - \rho(\mathrm{Ru}) - \rho(\mathrm{H_2O}) \qquad (2)$$

reveals the redistribution of charge upon adsorption. This is shown in Figure 8a and it clearly illustrates the role played by the $\mathbf{1b_1}$ and Ru $\mathbf{d_{z^2}}$ states. A remarkably clear depletion of the $\mathbf{1b_1}$ and Ru $\mathbf{d_{z^2}}$ orbitals is seen with charge accumulation in other regions (Ru $\mathbf{d_{xz}}$ and $\mathbf{d_{yz}}$ orbitals and on O) and a small charge accumulation in the internuclear region between O and Ru. This suggests that the antibonding states formed by the $\mathbf{1b_1}$−$\mathbf{d_{z^2}}$ mixing have transferred electrons into the lower-lying ($\mathbf{d_{xz}}$ and $\mathbf{d_{yz}}$) manifold.

(b) Intact Bilayer Adsorption. We now examine the adsorption of the most stable (H-up) intact H_2O bilayer on Ru. Two key features of the electronic structure in this system have been identified. These are best illustrated through the electron density difference plot, shown in Figure 8b. The electron density difference upon intact bilayer adsorption was calculated in a manner similar to the isolated H_2O molecule, that is, from the electron density of the adsorption system the electron densities of the Ru substrate and an isolated H_2O bilayer both in their optimized geometries obtained in the adsorption system were subtracted:

$$\rho(\mathrm{Ru} + \mathrm{H_2O\ bilayer}) - \rho(\mathrm{Ru}) - \rho(\mathrm{H_2O\ bilayer}) \qquad (3)$$

The first piece of information to be gleaned from Figure 8b is the complete absence of any charge redistribution upon adsorption around the higher-lying H_2O molecule in an intact bilayer. This is clear from Figure 8b for an isosurface of constant electron density of $\pm 0.03\ e/\text{Å}^3$. However, this is still true at lower densities and indeed it is only just above the level of the noise in the difference calculation that any redistribution of electron density about the higher-lying H_2O is detected. The negligible change in the electron density of the higher-lying

(36) The partial density of states (PDOS) analyses are performed by projecting the plane wave states onto a localized basis set by the projection technique of Sanchez-Portal. See Sanchez-Portal, D.; Artacho, E.; Soler, J. M. *Solid State Commun.* **1995**, *95*, 685.

(37) Hoffmann, R. *Solids and Surfaces: A Chemist's View of Bonding in Extended Structures*; VCH: New York, 1988.

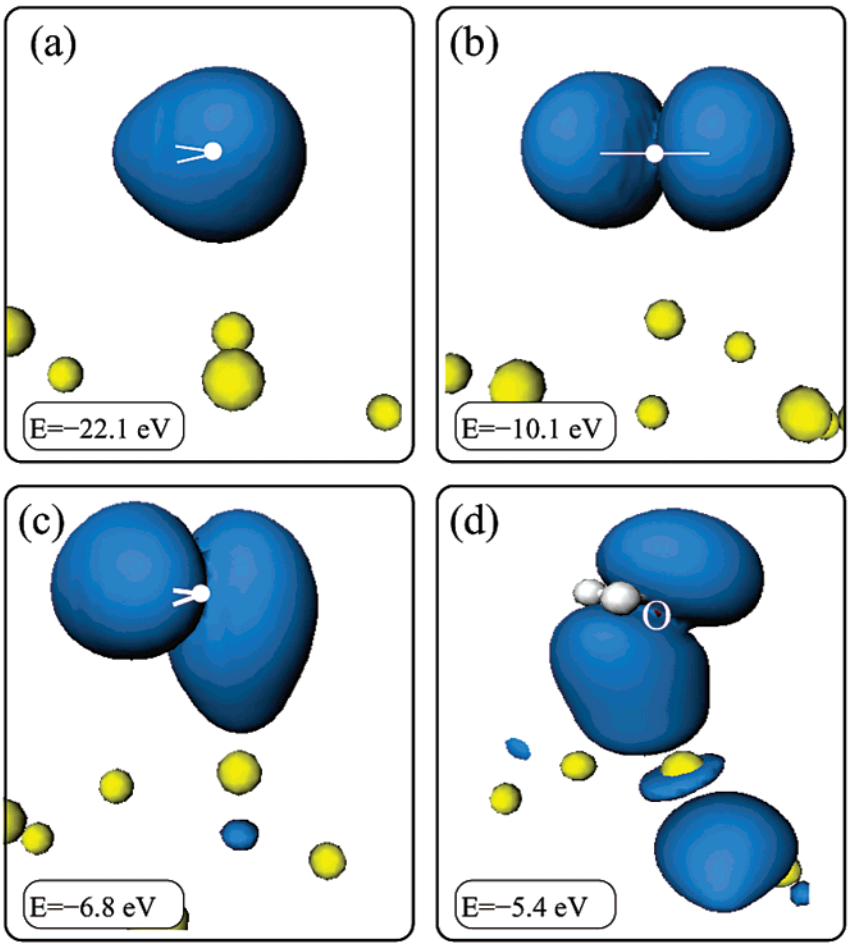

Figure 7. Isosurfaces of constant electron density (2×10^{-2} e/Å^3) for quantum states in the H_2O monomer adsorption system. The approximate energies of these states beneath the Fermi level are also given. (a) and (b) are $\mathbf{2a_1}$ and $\mathbf{1b_2}$ derived states, respectively. (c) is an example of a $\mathbf{3a_1}-\mathbf{d_{z^2}}$ mixed orbital state and (d) illustrates $\mathbf{1b_1}-\mathbf{d_{z^2}}$ mixing.

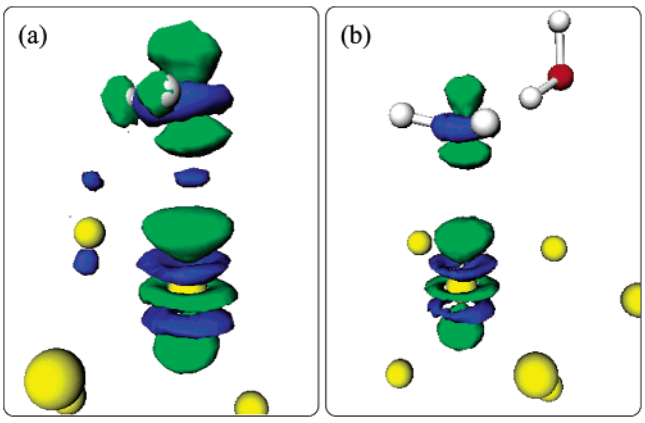

Figure 8. Isosurfaces of the difference electron density upon adsorption for (a) H_2O monomer adsorption and (b) H-up intact bilayer adsorption. Blue contours indicate an electron density increase of 3×10^{-2} e/Å^3; green contours indicate an electron density decrease of 3×10^{-2} e/Å^3.

H_2O molecule is remarkable and implies that, in an adsorbed bilayer, the higher-lying set of H_2O molecules do not bond directly to the surface. Although this finding has often been predicted,[6,7] Figure 8b provides the first clear evidence. It also implies that the electron redistribution on the lower-lying H_2O molecules (which do bond to the surface) does not affect the electron density of the higher-lying H_2O molecules.

Also apparent from Figure 8b is that the charge redistribution about the lower-lying H_2O and the Ru atom directly beneath it is very similar to that shown in Figure 8a for the adsorption of the H_2O monomer. This indicates that the low-lying H_2O molecules in a bilayer bond with the surface in a fashion similar to the isolated H_2O monomer. As is clear from figure 8a and b and confirmed through careful inspections at other density thresholds, the extent of charge redistribution is slightly less for the low-lying H_2O in a bilayer than it is for the adsorption of a H_2O monomer. This, as well as a longer H_2O-Ru bond, indicates that, although the bonding mechanism is similar, the H_2O-Ru bond for the lower-lying H_2O molecules in a bilayer is slightly weaker than the H_2O-Ru bond for the monomer.

The absence of a direct bond between the high-lying H_2O molecules and the surface is important because we can now make the first quantitative estimate of the strength of H bonding in an adsorbed bilayer. The adsorption energy of a single H_2O monomer in a $(\sqrt{3} \times \sqrt{3})$R30° unit cell is 0.35 eV (cf. 0.38 eV in a p(2 × 2) cell) and in a H-up bilayer the H_2O adsorption energy is 0.58 eV/H_2O. Thus, on formation of a bilayer from a $(\sqrt{3} \times \sqrt{3})$R30° overlayer of H_2O monomers, 0.81 eV is gained, which is about 70% of the total H_2O adsorption energy for the two H_2O molecules in the $(\sqrt{3} \times \sqrt{3})$ unit cell. Since there is no net increase in the amount of H_2O-Ru bonding,[38] this energy

(38) In fact, as we have just seen there appears to be a small decrease in H_2O-Ru bonding on going from the monomer to the bilayer adsorption systems.

gain is due entirely to H bond formation. Given that there are three H bonds per ($\sqrt{3} \times \sqrt{3}$)R30° unit cell, then the *average* H bond strength in the bilayer is $\geq$0.27 eV. This estimate is very similar to a recent DFT estimate for the H bond strength ($\geq$0.26 eV) for an adsorbed H_2O dimer on Pt{111}.[16]

4.2 Monomer versus Bilayer Dissociation. Arguably, the most important finding in this study is the ease with which the dissociation of a H_2O molecule incorporated in a bilayer is seen to proceed. We have learned that it is more inclined to do so in that state than it is as an isolated monomer. The barriers identified are, in the larger (3×3) and ($2\sqrt{3} \times 2\sqrt{3}$) unit cells, 0.85 and 0.50 eV for H_2O monomer and bilayer dissociation, respectively. When considered in terms of the relative *rate* of each dissociation process, the significance of this barrier difference becomes immediately apparent. Assuming standard Arrhenius parameters and a surface temperature of 150 K, a simple estimate of the relative rates of each process reveals that the dissociation rate in the bilayer should exceed that of the monomer by *twelve* orders of magnitude.

Aside from the lower kinetic barrier, it is also thermodynamically more favorable to dissociate in the bilayer. This releases 0.85 (0.40) eV (Figure 5) while dissociation of the H_2O monomer releases only 0.27 (0.00) eV (Figure 2) going to the separately adsorbed (coadsorbed) final states in each case. It is well known that the activation energy and the enthalpy change of a given reaction are often related.[39,40] Relationships of this sort are known as *linear free energy* or *Bronsted−Evans−Polanyi* relationships and have recently been shown to apply generally to surface reactions, including dehydrogenation reactions.[41−43] Essentially these relationships reveal that, all other things being equal, the greater the thermodynamic driving force for a reaction the lower its barrier will be. Assuming this is true for the systems under consideration here, a key issue to address then is why bilayer dissociation is thermodynamically more favorable than monomer dissociation. Since we are dealing with the same elementary step in both reactions (H_2O dissociation), it is not immediately clear, however, why one should release more energy than the other. A comparison of the various initial and final states helps to reveal a possible answer.

On going from the intact bilayer to the partially dissociated overlayer, the adsorbate−substrate and adsorbate−adsorbate bonding is altered. These changes contribute to the enthalpy change for the reaction. Although impossible to explicitly distinguish between them, it is of some value to estimate their relative importance. In the intact bilayers (initial state), the low-lying H_2O molecules bind to the surface, while the high-lying H_2O molecules, held in place through H bonding, do not. In contrast, in the OH−H_2O overlayer (final state) OH and H and also H_2O bind to the surface. Thus, the dissociation process in the bilayer actually resembles *dissociative adsorption*, that is, a H_2O that was not already chemisorbed on the surface has dissociated. This is clearly different from the dissociation of the chemisorbed monomer. Given that we calculate the chemisorption energy of a single H_2O monomer on Ru{0001} to be 0.35−0.38 eV (depending on the unit cell, see Table 1), the absence of a bond between the high-lying H_2O and the surface amounts to an effective destabilization of the bilayer initial state by approximately 0.35−0.38 eV. This relative decrease in the intact bilayer adsorbate−substrate bonding is the main contributor to the enhancement in the enthalpy change for dissociation in the bilayer. We suggest that any remaining enhancement in the enthalpy change may be accounted for by increased H bonding in the OH−H_2O overlayer compared to the intact bilayers. The structural parameters of the partially dissociated overlayer (Table 3) provide evidence for this. The OH−H_2O overlayer exhibits the two longest O−H bonds (1.02 Å) and two of the shortest H···O hydrogen bonds (1.64 and 1.67 Å) in any overlayer examined.

Facile H_2O dissociation in a bilayer may be important because it can have more general applications. Indeed, it is likely not to be specific to H_2O bilayers but to also apply to H-bonded H_2O clusters and even to other H-bonded overlayers (for example, H_2S or amino acid overlayers). The findings here suggest that there may be an enhanced thermodynamic driving force for dissociation of a molecule in a H-bonded overlayer if (i) the molecule is not already bonding with the surface and (ii) dissociation brings about an increase in H bonding or at least does not result in a loss of H bonding. Indeed, this helps to reveal why the dissociation of H_2O in the OH−H_2O overlayer (to produce the fully dissociated 2OH overlayer) is thermodynamically unfavorable (Figure 5). In this dissociation process, H_2O is already chemisorbed on the surface. In addition, the number of H bonds per ($\sqrt{3} \times \sqrt{3}$) cell is reduced from three to two.

4.3 The Issue of the Partially Dissociated Overlayer. Finally, we briefly consider what implications our results have for the possibility of a partially dissociated overlayer on Ru. In agreement with Feibelman,[1] we have found that the partially dissociated OH−H_2O overlayer is more stable than any pure H_2O overlayers and provides good agreement with Held and Menzel's structure[12] that forms upon D_2O adsorption on Ru. We have also ruled out a "fully dissociated" OH overlayer as a candidate structure. Further, a mechanism, with a barrier of 0.5 eV, for the formation of a partially dissociated overlayer from an intact bilayer has been identified. Given this, we are inclined to agree with Feibelman's interpretation that the structure of the first H_2O layer on Ru is a partially dissociated OH−H_2O overlayer.

Since the barrier to dissociate a H_2O incorporated in an intact bilayer is much less than that for an isolated H_2O monomer, it appears that on a mesoscopic length scale intact H_2O molecules adsorb, arrange into H_2O clusters or partial intact bilayers, and then dissociate into the partially dissociated overlayer. Although dissociation of H_2O monomers through alternative routes (for example, at defect sites on the surface) cannot been ruled out, the magnitude of this barrier strongly suggests that isolated chemisorbed H_2O molecules should not dissociate at low temperatures on Ru{0001} terraces. Moreover, there is some experimental evidence that H_2O dissociation in H_2O clusters takes place between 100 and 170 K on Ru{0001}.[4] Our barrier of 0.5 eV is compatible with dissociation at an appreciable rate at the higher end of this temperature range.

Finally, the addition of zero point energy corrections to our obtained barriers would require calculation of vibrational

(39) Shorter, J. *Correlation Analysis in Organic Chemistry: An Introduction to Linear Free Energy Relationships*; Clarendon Press: Oxford, 1973.
(40) Masel, R. I. *Principles of Adsorption and Reaction at Solid Surfaces*; Wiley-Interscience: New York, 1996.
(41) Liu, Z.-P.; Hu, P. *J. Chem. Phys*. **2001**, *115*, 4977.
(42) Logadottir, A.; Rod, T. H.; Nørskov, J. K.; Hammer, B.; Dahl, S.; Jacobsen, C. J. H. *J. Catal*. **2001**, *197*, 229.
(43) Michaelides, A.; Liu, Z.-P.; Zhang, C. J.; Alavi, A.; King, D. A.; Hu, P. *J. Am. Chem. Soc.*, accepted.

frequencies, which we have not done. However, it is likely that both the monomer and the bilayer dissociation barriers will be reduced somewhat. Owing to the lighter mass of H than D, this reduction is likely to be more pronounced for H_2O dissociation compared to D_2O dissociation. Unfortunately, at present we are not able to give an estimate of the importance of these effects.

5. Summary & Conclusions

The first comparative theoretical study of the adsorption and dissociation of H_2O monomers and icelike bilayers on a metal surface has been performed. Some of the key findings and implications of this work are now briefly recapped.

(i) H_2O monomers bind preferentially at atop sites, with an adsorption energy of $\sim$0.4 eV.

(ii) The H_2O-Ru bonding interaction is mainly through $\mathbf{1b_1}-\mathbf{d_{z^2}}$ mixed orbital states. Some weak $\mathbf{3a_1}-\mathbf{d_{z^2}}$ mixing has also been identified.

(iii) In an intact bilayer, the low-lying set of H_2O molecules bind through a similar mechanism to the H_2O monomer. Evidence has been presented to show that the high-lying H_2O molecules do not bond with the surface.

(iv) In agreement with Feibelman's recent DFT study, we find that a partially dissociated $OH-H_2O$ overlayer is (i) thermodynamically more stable than any pure H_2O bilayers identified and (ii) provides very good structural agreement with Held and Menzel's experimental structure for D_2O adsorption on Ru. We have also identified a mechanism for the formation of the partially dissociated overlayer with a barrier of just 0.5 eV. Given the weight of evidence, we conclude that a partially dissociated overlayer is the best candidate for the current experimental structure.

(v) The activation energy for the dissociation of a H_2O monomer is about 0.8 eV. This suggests that isolated chemisorbed H_2O molecules should not dissociate at low temperatures on Ru{0001} terraces.

(vi) Finally, our calculations reveal that it is substantially easier to dissociate a H_2O incorporated in a H_2O bilayer than it is to dissociate a chemisorbed H_2O monomer. The particular details of this explanation can have more general applications to other H-bonded systems which we have highlighted.

Acknowledgment. This work has been supported by EPSRC. A. M. wishes to thank Gonville and Caius College, Cambridge for a research fellowship. The Cambridge High Performance Computing Facility is gratefully acknowledged for computing time. Drs. Pedro deAndres, Georg Held, and Stephen Jenkins and Mr. Sakari Puisto are thanked for helpful discussions.

JA028855U